Photodissociation Dynamics of 1-Bromo-1-chloro-2,2,2-trifluoroethane at 157 nm

Atsushi Yokoyama,*,† Keiichi Yokoyama,† and Toshiyuki Takayanagi‡

Department of Chemistry and Fuel Research and Advanced Science Research Center, Japan Atomic Energy Research Institute, Tokai-mura, Naka-gun, Ibaraki-Ken 319-11, Japan

Received: February 18, 1997; In Final Form: April 22, 1997[⊗]

The photodissociation dynamics of the title molecule at 157 nm has been studied using photofragment translational spectroscopy. The molecule was found to dissociate competitively via $CHBrCF_3 + Cl$, $CHClCF_3 + Br$, $CHCF_3 + Br + Cl$, and $CClCF_3 + HBr$ channels with the branching ratio $1.0{:}0.75^{+0.19}_{-0.00}{:}0.40^{+0.40}_{-0.20}{:}0.55^{+0.55}_{-0.28}$. This result indicates that the stronger C−Cl bond breaks preferentially over the weaker C−Br bond, similar to the case of the photodissociation of $CBrF_2CHClF$ studied previously. Compared with the C−Cl:C−Br branching ratio ($1.0{:}0.27^{+0.15}_{-0.04}$) for the photodissociation of $CBrF_2CHClF$ at 157 nm, this branching ratio indicates that a larger fraction of molecules dissociate via C−Br bond rupture in this case than in the case of $CBrF_2CHClF$ as a result of a higher transition probability from the initially excited nσ*(C−Cl) diabatic surface to the nσ*(C−Br) diabatic surface. This result is qualitatively consistent with the prediction from previous theoretical works that the transition probability from the nσ*(C−Cl) to the nσ*(C−Br) diabatic surface increases with decreasing spatial distance between the Br and Cl atoms. The secondary dissociation of $CHBrCF_3$ and $CHClCF_3$ was also observed following 1,2-fluorine migration. This mechanism was supported by an energy diagram obtained by ab initio molecular orbital (MO) calculations at the QCISD(T) level of theory. The dynamics of the triple dissociation, $CHCF_3 + Br + Cl$, is discussed using the potential energy surfaces of CH_2BrCl constructed by ab initio MO calculations.

Introduction

There has been considerable interest in bond-selective chemistry in recent years. The preferential dissociation of a stronger carbon−halogen bond over a weaker bond has been observed following direct excitation to an antibonding orbital of the stronger bond. Butler et al. reported the preferential C−Br bond rupture over the weaker C−I bond in the ultraviolet photodissociation of CH_2BrI[1] and $CH_2BrCH_2CH_2I$.[2] We also observed the preferential C−Cl bond rupture over the weaker C−Br bond in the vacuum ultraviolet photodissociation of $CBrF_2CHClF$.[3]

Butler and co-workers pointed out that nonadiabatic transition between electronic excited states plays an important role in determining the branching ratios of competitive dissociation reactions in their works on the photodissociation of several ketones following local ^{1}[n,π*(C=O)] excitation.[4−6] The situation is also true for the competitive C−halogen bond ruptures following local nσ*(C−halogen) excitation. We have examined theoretically the effect of the coupling strength between the nσ*(C−Cl) and nσ*(C−Br) diabatic surfaces on the branching ratio of C−Cl bond rupture to C−Br bond rupture by using wavepacket calculations.[7] A fraction of the C−Br bond rupture was found to increase with increasing coupling strength as a result of the increase in the transition probability from the locally excited nσ*(C−Cl) diabatic surface to the nσ*(C−Br) diabatic surface. The coupling strength between the diabatic surfaces was found to be approximately proportional to the splitting between the adiabatic surfaces, resulting from the avoided crossing of the diabatic surfaces. According to our recent ab initio MO calculations of the splitting between two singlet adiabatic potential energy surfaces, the magnitude of the splitting depends on the molecular structure; i.e., the coupling strength, in most cases, becomes larger with a decrease of the spatial distance beween the Cl and Br atoms.[8] Therefore, it is expected that a molecule in which a Br atom and a Cl atom are attached to the same C atom dissociates via C−Br bond rupture with a higher branching fraction than that for a molecule in which a Br atom and a Cl atom are attached to different C atoms, because the distance between the Br and Cl atoms is shorter in the former molecule.

In this paper, we present the photodissociation mechanism and dynamics of $CHBrClCF_3$ at 157 nm to examine the effect of the molecular structure on the selective C−Cl bond dissociation. Since no absorption spectrum of this molecule has been reported, an exact assignment of the transition at 157 nm could not be done. The absorption spectrum of $CBrClF_2$[9] shows a peak attributed to the n(Cl) → σ*(C−Cl) transition at around 164 nm. A peak in the absorption band corresponding to the Rydberg transition n(Br) → 5s appears at a wavelength shorter than about 150 nm. Therefore, the initial excitation of $CHBrClCF_3$ at 157 nm would be assigned to be the n(Cl) → σ*-(C−Cl) transition.

Experimental Section

Time-of-flight (TOF) spectra of dissociation products were measured by a cross-laser and molecular-beam technique using a rotating molecular-beam-source apparatus. The molecular-beam apparatus used in this experiment was described previously.[10] Briefly, the Ar-seeded $CHBrClCF_3$ beam was produced by expanding a $CHBrClCF_3$/Ar mixture at a stagnation pressure of 300 Torr into the source chamber through a nozzle heated at 110 °C. An F_2 laser (Lambda Physik LPF-205) was used as the light source. A laser pulse with a pulse energy of 70 mJ was focused to a 1×3-mm^2 spot at the interaction region of the laser and the molecular beam. We also measured the TOF spectra by irradiating the $CHBrClCF_3$ beam with the unfocused laser beam whose spot size was 5×15 mm^2. The laser was operated at 50 Hz. The dissociation products were detected at a beam-to-detector angle of 20° by a triply differentially pumped

† Department of Chemistry and Fuel Research.
‡ Advanced Science Research Center.
⊗ Abstract published in *Advance ACS Abstracts,* July 1, 1997.

S1089-5639(97)00601-4 CCC: $14.00

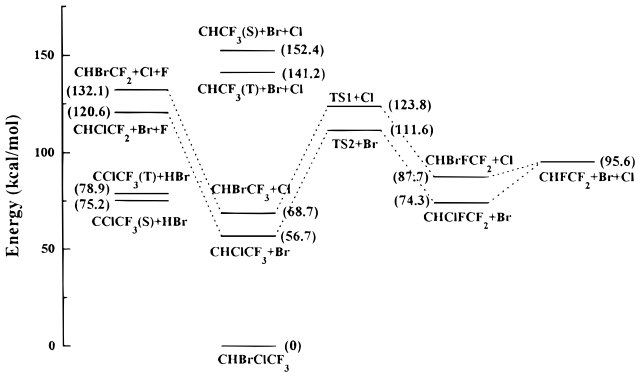

Figure 1. Potential energy diagram for the dissociation of $CHBrClCF_3$, constructed by the ab initio MO calculations at the QCISD(T) level of theory. Values in parentheses are the enthalpy changes from the ground-state $CHBrClCF_3$ in units of kcal/mol. TS1 and TS2 denote the transition states for the 1,2-fluorine migrations of $CHBrCF_3$ and $CHClCF_3$, respectively. T and S stand for the triplet and singlet states, respectively.

quadrupole mass spectrometer (Extrel C-50) after ionization by electron bombardment at 100 eV in the ionizer located 44.0 cm away from the interaction region of the laser and the molecular beam.

Computation of Enthalpy Changes. In order to assist the analysis of experimental data and discussion of results, enthalpy changes associated with the reactions expected to occur were calculated by the ab initio MO method. The calculations were done using Gaussian 94[11] at the MP2(full) level of theory to compute the optimized geometries and vibrational frequencies of the equilibrium structures and transition states for 1,2-fluorine migration of $CHClCF_3$ and $CHBrCF_3$. Single-point energies for the optimized geometries were calculated at the QCISD(T) level of theory. Dunning and Huzinaga's double-ζ-plus polarization (DZP) basis functions[12] were used for the H, C, and F atoms, while the effective core potential developed by Hay and Wadt was used with split valence and polarization functions[13] for the Cl and Br atoms. Figure 1 shows the energy diagram constructed from the calculations.

Results

Signals were detected at $m/e = 35$ ($^{35}Cl^+$), 79 ($^{79}Br^+$), 80 ($H^{79}Br^+$), and 82 ($C_2F_3H^+$ and $H^{81}Br^+$). The shapes of the TOF spectra obtained with the focused laser beam are the same as those obtained with the unfocused laser beam whose intensity is $^1/_{25}$th of the intensity of the focused laser beam. Therefore, the multiphoton processes are not important even at the highest laser intensity used. TOF spectra are shown in Figure 2. The fast sharp peak in the spectrum at $m/e = 35$ shown in Figure 2a is attributed to Cl atoms produced by the following C−Cl bond rupture:

$$CHBrClCF_3 \rightarrow CHBrCF_3 + Cl \qquad (1)$$

The center-of-mass (c.m.) translational energy distribution for this reaction was obtained by fitting this spectrum by a forward convolution method[14] and is shown in Figure 3a. The fast peak in the TOF spectrum at $m/e = 79$ shown in Figure 2b is attributed to Br atoms produced by the following C−Br bond rupture:

$$CHBrClCF_3 \rightarrow CHClCF_3 + Br \qquad (2)$$

The c.m. translational energy distribution for this reaction is shown in Figure 3b. Since the c.m. translational energy distributions for reactions 1 and 2 peak at high translational energies, which is typical for a carbon−halogen bond rupture on a repulsive potential energy surface, these reactions should occur via the nσ^*(C−Cl) and nσ^*(C−Br) surfaces, respectively.

The internal energies of the $CHBrCF_3$ products from reaction 1 are estimated to range from 56 to 107 kcal/mol from the excitation energy (181.3 kcal/mol), the C−Cl bond dissociation energy of $CHBrClCF_3$ (68.7 kcal/mol), and the c.m. translational energy distribution for reaction 1. Similarly, the internal energies of the $CHClCF_3$ products from reaction 2 are estimated to range from 69 to 121 kcal/mol with the calculated C−Br bond dissociation energy (56.7 kcal/mol). Most of the internal energies of the $CHBrCF_3$ and $CHClCF_3$ products exceed the enthalpy changes at 0 K for the following C−F bond ruptures of $CHBrCF_3$ (63.4 kcal/mol) and $CHClCF_3$ (63.9 kcal/mol):[15]

$$CHBrCF_3 \rightarrow CHBr{=}CF_2 + F \qquad (3a)$$

and

$$CHClCF_3 \rightarrow CHCl{=}CF_2 + F \qquad (3b)$$

The enthalpy changes for these reactions are lower than those for the following C−Br bond rupture of $CHBrCF_3$ (72.5 kcal/mol) and C−Cl bond rupture of $CHClCF_3$ (84.5 kcal/mol):

$$CHBrCF_3 \rightarrow CHCF_3 + Br \qquad (4a)$$

and

$$CHClCF_3 \rightarrow CHCF_3 + Cl \qquad (4b)$$

where the $CHCF_3$ product should be in the triplet state, which is 11.2 kcal/mol lower than the singlet state. Therefore, most of the radicals would have dissociated through C−F bond ruptures if no 1,2-fluorine migration occurred. However, neither F, $CHBrCF_2$, nor $CHClCF_2$ could be detected. Instead, slow Br and Cl atoms were detected as shown in Figure 2. If these reactions occurred via reactions 4a and 4b, 65% of $CHBrCF_3$ and 37% of $CHClCF_3$ would have been stable. However, neither $CHBrCF_2^+$, $CHClCF_2^+$, $CHBr^+$, nor $CHCl^+$ signal supporting the existence of these stable radicals was detected. Thus, the Br and Cl atoms should come from other channels having lower threshold energies. Possible candidates are C−Br bond rupture of $CHBrFCF_2$ and C−Cl bond rupture of $CHClFCF_2$ following 1,2-fluorine migration:

$$CHBrCF_3 \rightarrow CHBrFCF_a \qquad (5a)$$

$$CHBrFCF_2 \rightarrow CHFCF_2 + Br \qquad (6a)$$

and

$$CHClCF_3 \rightarrow CHClFCF_2 \qquad (5b)$$

$$CHClFCF_2 \rightarrow CHFCF_2 + Cl \qquad (6b)$$

If the activation energies for reactions 5a and 5b are lower than those for reaction 3, the spontaneous dissociation of the $CHBrCF_3$ and $CHClCF_3$ products occurs via reactions 6a and 6b following reactions 5a and 5b. The activation energies for reactions 5a and 5b were calculated to be 55.1 and 54.9 kcal/mol, respectively. Since these values are about 8−9 kcal/mol lower than the enthalpies for reactions 3a and 3b, the spontaneous dissociation of the $CHBrCF_3$ and $CHClCF_3$ products should occur via reactions 5a, 5b, 6a, and 6b. The contribution of the Cl atoms from reaction 6b is shown as the dotted line in Figure 2a and the contribution of the Br atoms from reaction 6a as the dashed line in Figure 2b. The contributions of $CHFCF_2$ from reactions 6a and 6b are shown as the dashed and dotted lines

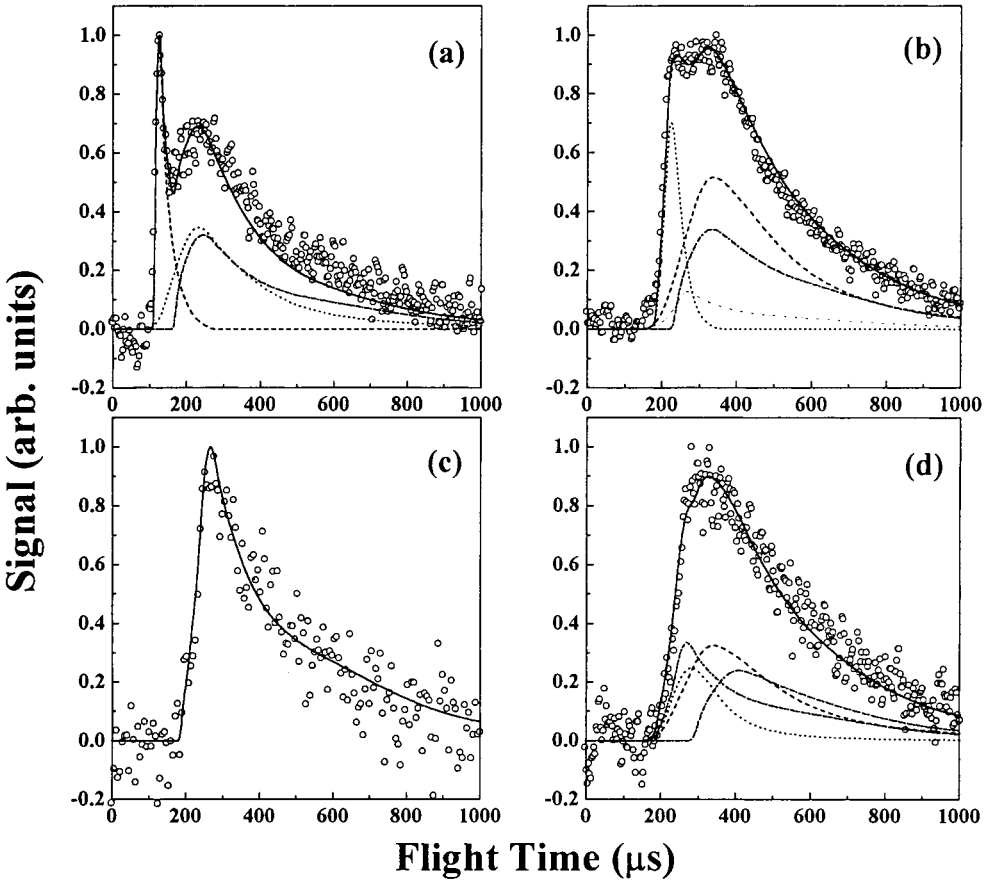

Figure 2. TOF spectra at (a) *m/e* = 35, (b) *m/e* = 79, (c) *m/e* = 80, and (d) *m/e* = 82. (a) (- - -) Contribution of Cl from reaction 1, (···) from reaction 6b, (− · −) from reaction 7. (b) (···) Contribution of Br from reaction 2, (- - -) from reaction 6a, (− · −) from reaction 7, (− ·· −) contribution of $H^{79}Br$ from reaction 8. (c) (—) Contribution of $H^{79}Br$ from reaction 8. (d) (- - -) Contribution of C_2HF_3 from reaction 6a, (···) from reaction 6b, (− · −) from reaction 7, (− ··−) contribution of $H^{81}Br$ from reaction 8.

in Figure 2d, respectively. The same c.m. translational energy distribution as shown in Figure 3e was used in the simulations for reactions 6a and 6b. Since the minimum internal energies of the $CHBrCF_3$ and $CHClCF_3$ products exceed the activation energies for the 1,2-fluorine migration of these products, all products can dissociate via reactions 6a and 6b. Therefore, the contribution of the Br atoms from reaction 6a in the TOF spectrum at *m/e* = 79 was determined so that the number of Br atoms from reaction 6a was equal to the number of Cl atoms from reaction 1. Similarly, the contribution of the Cl atoms from reaction 6b in the TOF spectrum at *m/e* = 35 was determined so that the number of Cl atoms from reaction 6b was equal to the number of Br atoms from reaction 2.

The slow components in the TOF spectra at *m/e* = 35, 79, and 82 could not be fit only with the reactions described above. The following triple dissociation reaction producing Br, Cl, and $CHCF_3$ products should also occur:

$$CHBrClCF_3 \rightarrow CHCF_3 + Br + Cl \qquad (7)$$

The best fit was obtained with 123° of the angle between the recoil vectors of the Cl and Br fragments and 136° of the angle between the recoil velocity of the Br and C_2HF_3 fragments. These angles are slightly different from the angles determined from the optimized geometry of $CHBrClCF_3$, which are 113° and 146°, respectively. The contributions of the Br, Cl, and $CHCF_3$ products from reaction 7 are shown as dash-dotted lines in parts a, b, and d of Figure 2, respectively. The c.m. translational energy distribution for reaction 7 is shown in Figure 3c. Hydrogen bromide is observed as $H^{79}Br^+$ and $H^{81}Br^+$ in the TOF spectrum at *m/e* = 80 and 82 as shown in parts c and d of Figure 2. The signal of this product is also observed as a $^{79}Br^+$ daughter ion of $H^{79}Br$ as shown in Figure 2b. This HBr product comes from the following HBr elimination from $CHBrClCF_3$:

$$CHBrClCF_3 \rightarrow CClCF_3 + HBr \qquad (8)$$

The c.m. translational energy distribution for reaction 8 is shown in Figure 3d.

The branching ratio between the primary dissociation processes was determined from the relative signal intensities of Br^+, Cl^+, and HBr^+ originating from Br, Cl, and HBr from reactions 1, 2, 7, and 8 by the procedure described in ref 17. The branching ratio of (1):(2):(7):(8) was determined to be 1.0: 0.75:0.4:0.55. In this estimation, the values of the anisotropy parameter β for all channels were assumed to be 0. However, β may not be 0 for dissociation processes on electronically excited potential energy surfaces. Moreover, the detection sensitivity of the products depends on the β values, even though the laser light is unpolarized. The products with the higher anisotropy parameters are detected with higher sensitivity by a factor of $1 + \beta/4$. Therefore, the uncertainty of the β values brings errors in the estimation of the branching ratio. In order to estimate the β values, we calculated the transition dipole moments for the third and fourth lowest excited singlet states, which are primarily characterized as the $n\sigma^*$(C−Cl) state. The complete active space self-consistent field (CASSCF) procedure implemented in MOLCAS-2[18] was used with DZP-quality basis sets. Details of the computation were described in ref 8. The angles between the transition dipole moments and the C−Cl bond are 43.7° and 22.4° for the third and fourth singlet states,

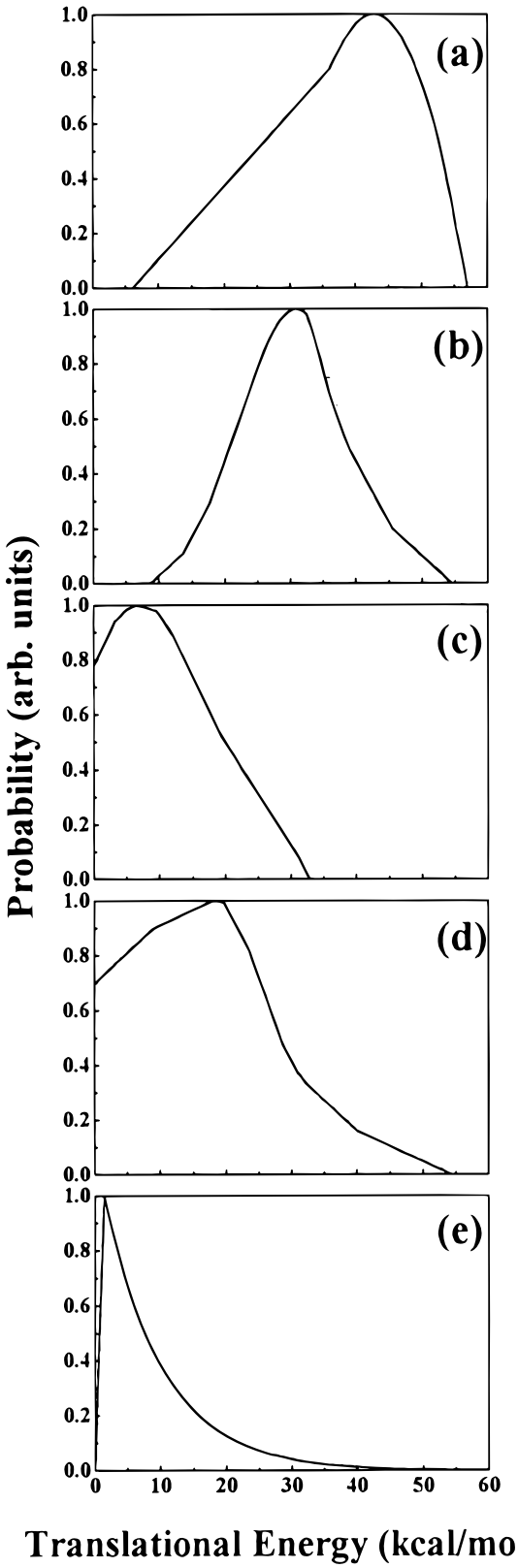

Figure 3. Center-of-mass translational energy distributions for (a) reaction 1, (b) reaction 2, (c) reaction 7, (d) reaction 8, and (e) reactions 6a and 6b.

respectively. Therefore, the β values for reaction 1 were calculated to be 0.566 and 1.563 in the case of the initial excitation to the third and fourth singlet states, respectively, from the definition of β:[19]

$$\beta = 2P_2(\cos \alpha)$$

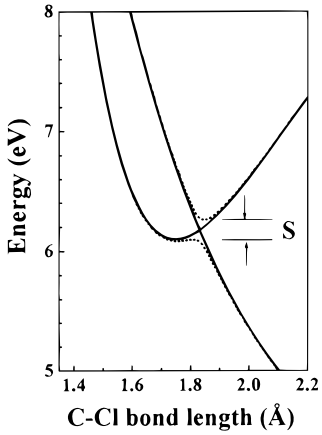

Figure 4. Schematic potential energy diagram for the definition of the splitting S between the adiabatic potentials (···) resulting from the avoided crossing of the diabatic potentials (—).

where P_2 denotes the second Legendre polynomial and α the angle between the transition dipole moment and the recoil direction of the Cl fragment in the c.m. system. The recoil direction of the Cl fragment was assumed to be the direction of the C−Cl bond. Similarly, the β values for reaction 2 were estimated to be 0.258 and 0.439 in the case of the initial excitation to the third and fourth singlet states, respectively. Therefore, the upper limit of the branching ratio of the C−Br bond rupture to the C−Cl bond rupture would be 0.94 with β values of 1.563 and 0.439 for reactions 1 and 2, respectively. If the molecule rotates or distorts during dissociation, the β values approach 0. Therefore, the branching ratio obtained by assuming a β value of 0 would be the lower limit. By taking the upper and lower limits of the β value, i.e., 2 and −1, as the β values for reactions 7 and 8, we obtained the branching ratio including errors originating from the uncertainty of the β values to be $1.0{:}0.75^{+0.19}_{-0.00}{:}0.40^{+0.40}_{-0.20}{:}0.55^{+0.55}_{-0.28}$.

Discussion

In the photodissociation of $CHBrClCF_3$ at 157 nm, the competitive C−Cl and C−Br bond ruptures were observed with a C−Cl:C−Br bond-rupture branching ratio of $1.0{:}0.75^{+0.19}_{-0.00}$. Compared with the C−Cl:C−Br bond-rupture branching ratio for $CBrF_2CHClF$ ($1.0{:}0.27^{+0.15}_{-0.04}$),[3,20] the branching ratio for $CHBrClCF_3$ indicates that the transition probability from the nσ*(C−Cl) diabatic surface to the nσ*(C−Br) diabatic surface would be larger for $CHBrClCF_3$ than for $CBrF_2CHClF$. As has been discussed in ref 3, the C−Br bond rupture would not be due to the direct excitation to the nσ*(C−Br) surface but is due to the transition from the nσ*(C−Cl) surface to the nσ*-(C−Br) surface. In our recent wavepacket calculations on the dissociation of CH_2BrCl on the nσ*(C−Cl) and nσ*(C−Br) diabatic surfaces,[7] it has been shown that the transition probability from the nσ*(C−Cl) surface to the nσ*(C−Br) surface depends on the coupling strength between the diabatic surface, which is approximately proportional to the splitting S (Figure 4) around the avoided crossing region between the adiabatic surfaces resulting from the avoided crossing between the nσ*-(C−Cl) and nσ*(C−Br) surfaces. As a result of the increase of the coupling strength, it was found that the fraction of C−Br bond rupture increases with increasing the magnitude of the splitting. From the recent ab initio calculations of the magnitude of the splitting between two $^1A'$ states and between two $^1A''$ state for several C_s-symmetric molecules with the CASSCF procedure,[8] the magnitude of the splitting was found to depend roughly on the spatial distance between the Br and Cl atoms in

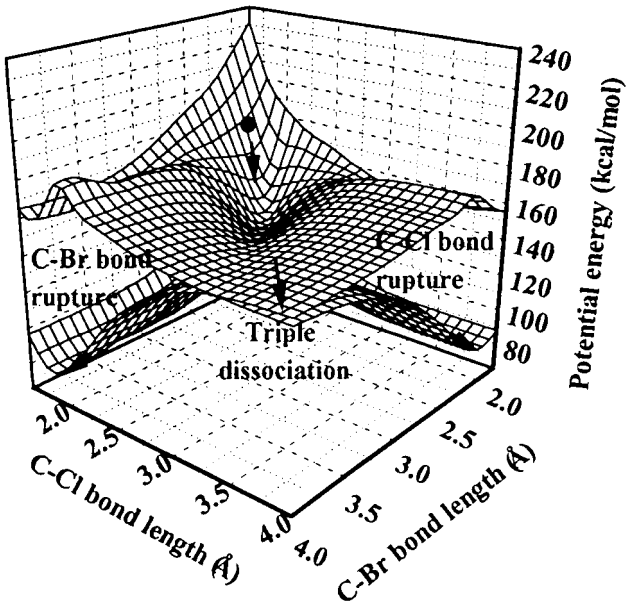

Figure 5. Potential energy surfaces for the lowest two 1A′ states of CH_2BrCl.

a molecule. For example, the magnitudes of the splitting are 1103, 517, 263, and 53 cm^{-1} respectively for the $^1A''$ states of CH_2BrCl, *anti*-C_2H_4BrCl, C_3H_6BrCl, and C_4H_8BrCl, in which the spatial distances between the Br and Cl atoms are 3.2, 4.6, 5.7, and 7.1 Å, respectively. In the case of the $^1A'$ states, the magnitudes of the splitting are 3624, 812, 1193, and 201 cm^{-1} for CH_2BrCl, *anti*-C_2H_4BrCl, C_3H_6BrCl, and C_4H_8BrCl, respectively. Therefore, the branching ratio of the C−Br bond rupture to the C−Cl bond rupture would be larger for $CHBrClCF_3$ than for $CBrF_2CHClF$, because the distance between Br and Cl in the former molecule is shorter than that in the latter molecule. This is consistent with the present experimental results. A similar tendency was also reported from the comparison of the branching ratio of the C−Br bond rupture to the C−I bond rupture for $CH_2BrCH_2CH_2I$ with that for $CBrF_2CF_2I$[21] and discussed from a similar point of view.[2]

Triple dissociation, reaction 7, also occurred in competition with the C−Cl and C−Br bond ruptures. In order to discuss the dynamics of the triple dissociation, we calculated the potential energy surface of the $^1A'$ state of CH_2BrCl by ab initio MO calculations using the CASSCF procedure with DZP-quality basis sets, because the calculation of the potential energy surfaces of $CHBrClCF_3$ is much more expensive. Spin−orbit couplings were not included in this calculation. The potential energy surfaces of the two lowest excited $^1A'$ states of CH_2BrCl are shown in Figure 5. A wavepacket indicated as the filled circle is initially created in the Franck−Condon region on the upper surface by photoexcitation. The wavepacket subsequently evolves downward on the surface. If the wavepacket jumps from the upper surface to the lower surface, the wavepacket moves either on the valley along the C−Cl coordinate to the $CHBrCF_3$ + Cl product or on the valley along the C−Br coordinate to the $CHClCF_3$ + Br product. On the other hand, if no transition from the upper surface to the lower surface occurs, the wavepacket moves along the diagonal valley to the product channel of the simultaneous C−Cl and C−Br bond ruptures. The transition probability from the upper surface to the lower surface decreases with increasing the splitting between the surfaces. The splitting would increase with decreasing the spatial distance between the Br and Cl atoms in a molecule as described before. Therefore, the chance that the wavepacket moves adiabatically on the upper surface to the product channel of the triple dissociation would increase for the molecule in which the Cl and Br atoms are attached to the same C atom similar to $CHBrClCF_3$. The triple dissociation producing the CF_2 + I + I product has also been reported in the photodissociation of CF_2I_2 at 308 and 248 nm.[22,23] The topology of the potential energy surface contributing the triple dissociation would be similar in both cases.

Conclusions

In the photodissociation of $CHBrClCF_3$ at 157 nm, the molecule dissociated competitively through C−Cl bond rupture, C−Br bond rupture, triple dissociation producing the product C_2HF_3 + Br + Cl, and HBr elimination with the branching ratio $1.0{:}0.75^{+0.19}_{-0.00}{:}0.40^{+0.40}_{-0.20}{:}0.55^{+0.55}_{-0.28}$. All $CHBrCF_3$ and $CHClCF_3$ radicals produced by the C−Cl and C−Br bond ruptures dissociated spontaneously via the C−Br and C−Cl bond ruptures following the 1,2-fluorine migration, respectively. Compared with the result of the photodissociation of $CBrF_2$-CHClF, this result indicates that the branching ratio of the C−Br bond rupture to the C−Cl bond rupture becomes larger as the spatial distance between the Br and Cl atoms is shorter. This tendency is consistent with the results of the theoretical calculations on the selectivity of the C−Cl bond rupture following the local excitation to the nσ^*(C−Cl) state, in which the transition probability from the nσ^*(C−Cl) diabatic surface to the nσ^*(C−Br) surface is shown to increase with decreasing spatial distance between the Br and Cl atoms.[7,8] The possibility of the triple dissociation would be supported by the characteristic of the calculated potential eneregy surface for the $^1A'$ state of CH_2BrCl, which indicates the triple dissociation occurs when the wavepacket moves adiabatically on the potential energy surface to which the molecule is initially excited.

References and Notes

(1) Butler, L. J.; Hintsa, E. J.; Shane, S. F.; Lee, Y. T. *J. Chem. Phys.* **1987**, *86*, 2051.
(2) Stevens, E. J.; Kitchen, D. C.; Waschewsky, G. C. G.; Butler, L. J. *J. Chem. Phys.* **1995**, *102*, 3179.
(3) Yokoyama, A.; Takayanagi, T.; Fujisawa, G. *J. Chem. Phys.* **1995**, *103*, 1710.
(4) Person, M. D.; Kash, P. W.; Butler, L. J. *J. Chem. Phys.* **1992**, *97*, 355.
(5) Kash, P. W.; Waschewsky, G. C. G.; Butler, L. J.; Francl, M. M. *J. Chem. Phys.* **1993**, *99*, 4479.
(6) Kash, P. W.; Waschewsky, G. C. G.; Morss, R. E.; Butler, L. J.; Francl, M. M. *J. Chem. Phys.* **1994**, *100*, 3463.
(7) Takayangi, T.; Yokoyama, A. *Bull. Chem. Soc. Jpn.* **1995**, *68*, 2225.
(8) Yokoyama, K.; Takayanagi, T.; Yokoyama, A. *J. Chem. Phys.*, submitted.
(9) Doucet, J.; Gilbert, R.; Sauvageau, P.; Sandorfy, C. *J. Chem. Phys.* **1975**, *62*, 366.
(10) Yokoyama, A.; Yokoyama, K.; Fujisawa, G. *J. Chem. Phys.* **1994**, *100*, 6487.
(11) Frisch, M. J.; Trucks, G. W.; Schlegel, H. B.; Gill, P. M. W.; Johnson, B. G.; Robb, M. A.; Cheeseman, J. R.; Keith, T.; Petersson, G. A.; Montgomery, J. A.; Raghavachari, K.; AlLaham, M. A.; Zakrzewski, V. G.; Ortiz, J. V.; Foresman, J. B.; Peng, C. Y.; Ayala, P. Y.; Chen, W.; Wong, M. W.; Andres, J. L.; Replogle, E. S.; Gomperts, R.; Martin, R. L.; Fox, D. J.; Binkley, J. S.; Defrees, D. J.; Baker, J.; Stewart, J. P.; HeadGordon, M.; Gonzalez, C.; Pople, J. A. Gaussian 94, Revision B.2, Gaussian, Inc., Pittsburgh, PA, 1995.
(12) Dunning, T. H., Jr.; Hay, P. J. *Modern Theoretical Chemistry*; Schaefer, H. F., III, Ed.; Plenum: New York, 1977; Vol. 3, Chapter 1.
(13) Wadt, W. R.; Hay, P. J. *J. Chem. Phys.* **1985**, *82*, 284.
(14) Zhao, X. Ph.D. Dissertation, University of California, Berkeley, 1988.
(15) Since the activation energy of F, Cl, or Br + ethylene reaction is less than 1 kcal/mol as described in ref 16, the C−F, C−Br, and C−Cl bond dissociation energies are almost the same as the respective enthalpy changes.
(16) Nathanson, G. M.; Minton, T. K.; Shane, S. F.; Lee, Y. T. *J. Chem. Phys.* **1989**, *90*, 6157 and references therein.
(17) Krajovich, D.; Huisken, F.; Zhang, Z.; Shen, Y. R.; Lee, Y. T. *J. Chem. Phys.* **1982**, *77*, 5977.
(18) Andersson, K.; Blomberg, M. R. A.; Fülscher, M. P.; Kellö, Y.; Lindh, R.; Malmqvist, P.-Å.; Noga, J.; Olsen, J.; Roos, B. O.; Sadlej, A. J.;

Siegbahn, P. E. M.; Urvan, M.; Widmark, P.-O. MOLCAS Version 2, University of Lund, Sweden, 1991.

(19) Busch, G. E.; Wilson, K. R. *J. Chem. Phys.* **1972**, *56*, 3638.

(20) The error in the branching ratio was reestimated from the theoretical β values for the C−Cl and C−Br bond ruptures. In order to obtain the theoretical β values, we calculated the transition dipole moments for the third and fourth excited singlet states using the CASSCF procedure. Then, the theoretical β values for the C−Cl bond rupture were calculated to be −0.282 and −0.322 for the third and fourth excited singlet states, respectively. The theoretical β values for the C−Br bond rupture were also calculated to be −0.765 and 1.768, respectively. The $CBrF_2CHClF$ geometry was assumed to be the gauche configuration in these calculations, because the error calculated from the transition dipole moments for *trans*-$CHBrClCF_3$ is smaller.

(21) Krajnovich, D.; Butler, L. J.; Lee, Y. T. *J. Chem. Phys.* **1984**, *81*, 3031.

(22) Wannenmacher, E. A. J.; Felder, P.; Huber, J. R. *J. Chem. Phys.* **1991**, *95*, 986.

(23) Baum, G.; Felder, P.; Huber, J. R. *J. Chem. Phys.* **1993**, *98*, 1999.